Catena 95 (2012) 112–123

Contents lists available at SciVerse ScienceDirect

Catena

journal homepage: www.elsevier.com/locate/catena

Aeolian sediment mass fluxes on a sandy soil in Central Patagonia

Geert Sterk [a,*], Jacopo Parigiani [b], Eduardo Cittadini [c], Piet Peters [d], Johannes Scholberg [e], Pablo Peri [f]

[a] Department of Physical Geography, Utrecht University, P.O. Box 80115, 3508 TC Utrecht, the Netherlands
[b] Green Resources Ltd, P.O. Box 55, Mafinga, Tanzania
[c] INTA-EEA Chubut, Ex-Ruta 25 km 1480, 9100 Trelew, Chubut, Argentina
[d] Land Degradation & Development group, Wageningen University, P.O. Box 47, 6700 AA Wageningen, the Netherlands
[e] Biological Farming Systems, Wageningen University, P.O. Box 563, 6700 AN Wageningen, the Netherlands
[f] UNPA-INTA-CONICET, INTA-EEA Santa Cruz, Chacra 45A, 9420 Río Gallegos, Santa Cruz, Argentina

ARTICLE INFO

Article history:
Received 24 March 2011
Received in revised form 4 January 2012
Accepted 8 February 2012

Keywords:
Argentina
Patagonia
Wind erosion
Windbreaks
Aeolian mass flux
Sediment transport equation

ABSTRACT

The climate of Patagonia is semi-arid and characterised by frequent strong winds. Wind erosion is potentially a serious soil degradation process that impacts long-term sustainability of local agricultural systems, but the conditions and the rates of wind erosion in this region have not been studied extensively. The aim of this study was to quantify windblown mass transport on a sandy soil in Central Patagonia. Aeolian mass fluxes were measured in the valley of Sarmiento (Chubut province, Argentina) using two saltiphones and 24 Modified Wilson and Cooke (MWAC) sediment catchers. The latter were installed along three transects: (1) a control on a bare strip of land cleared of its natural vegetation, to measure the maximum wind erosion; (2) a similar transect protected by an artificial windbreak with an optical porosity of 50%; and (3) a transect in a cherry orchard protected with the same type of windbreak. Nine windstorms were recorded throughout the experimental period. Storms with wind speed peaks of 20 m s^{-1} caused a total soil loss of 248 Mg ha^{-1} in the control strip and heavily depleted the soil of its erodible fraction. The artificial windbreak reduced the soil loss by 51.0% on average, while no erosion was recorded in the cherry orchard. Measured maximum mass transport values were used to fit five sediment transport equations in order to select the best equation to integrate into a GIS-based wind erosion prediction system. The Kawamura (1964) equation showed the highest model efficiency and was considered to be the best sediment transport equation for the Patagonia conditions. It expresses total mass transport as a function of two empirical constants: the threshold friction velocity (u_{*t}), and an erodibility coefficient C_{Ka}. It is concluded that wind erosion in Central Patagonia poses a serious risk of soil degradation once the natural vegetation is removed due to overgrazing or other anthropogenic activities.

1. Introduction

Patagonia is the southernmost region of South America, with the Andes dividing its Chilean and Argentinean sections. The Argentinean part of Patagonia extends from about 37° to 57° S. This region is covering 28.2% of the total national area with only 4.5% of the country's population, thus having a very low population density (1.9 inhabitants per km²) (Naumann, 1999). Patagonia presents a variety of ecosystems and climates and the main ecosystem is a semi-desert steppe. Rainfall is not strictly seasonal (Laya, 1981), but a high proportion of it usually occurs in small events during the winter (May–August) (Soriano, 1992). The distance from the Andes determines a spatial rainfall gradient and for each kilometre eastward of the mountain range, annual rainfall is being reduced by 7 mm (Paruelo et al., 1998). Argentinian Patagonia can therefore be divided in two sectors: the Andes and the plateau (Coronato and Bisigato, 1998). The Andes sector receives up to 1200 mm of rain per year (Naumann, 1999), enabling an abundant animal life and a luxuriant vegetation, and giving rise to the Ando-Patagonian forests. This region also provides excellent conditions for the production of forage, timber, fruits and horticultural crops (Dimitri, 1972).

The plateau is a semi-arid environment with annual precipitation ranging between 200 and 500 mm (León et al., 1998; Naumann, 1999). The ecosystem on the plateau is a semi-desert steppe, which covers roughly 85% of the area and is mainly used for extensive sheep grazing. The Patagonian plateau is incised by valleys running from West to East. These valleys represent only a small fraction of the area (≈1.5%) but provide more favourable living conditions, and hence the main urban centres are concentrated here. The valleys are widely used for more intensive and/or irrigated agricultural production systems. Major agricultural activities include sheep and beef cattle rearing, cultivation of alfalfa, wheat, potato and vegetables, as well as fruit orchards (Cittadini, 2007).

One of the most striking meteorological phenomena in Patagonia is the strong winds. Severe and frequent wind storms occur mainly

* Corresponding author at: Department of Physical Geography, Utrecht University, P.O. Box 80115, 3508 TC Utrecht, the Netherlands. Tel.: +31 30 2533051; fax: +31 30 2531145.
E-mail address: g.sterk@uu.nl (G. Sterk).

0341-8162/$ – see front matter © 2012 Elsevier B.V. All rights reserved.
doi:10.1016/j.catena.2012.02.005

during spring and summer (October–February), with wind speeds regularly exceeding 120 km h^{-1}. Such wind storms may last several days, often causing problems for traffic, air planes and buildings. Potentially, the wind storms could cause appreciable aeolian sediment transport especially on unprotected soils. When the protective soil cover by the steppe vegetation is removed, either by human activities or overgrazing by sheep, soils become exposed and may be eroded by the wind. According to Peri and Bloomberg (2002), overgrazing has already caused the degradation of more than 6.5 million hectares in Patagonia. Earlier, it was estimated that more than 30% of the surface in the region between the 41st parallel and the Magellan strait is affected by severe wind and water erosion (Pelliza et al., 1997). The constant presence of strong winds has resulted in extensive use of approximately 1500 km of windbreaks in the irrigated valleys of Patagonia to protect crops from wind damage as related to desiccation and sandblasting associated with wind erosion processes (Peri and Bloomberg, 2002).

Wind erosion is the process whereby soil particles are lifted and carried away by the wind. In the wind erosion process three transport modes can be distinguished: creep, saltation and suspension (Bagnold, 1941). Creep is the rolling or sliding movement of the larger (>~500 μm) particles that are too heavy to be lifted by the wind. Saltation transports fine to medium sized sand particles (~50–~500 μm). These particles bounce over the soil surface, reaching maximum heights of about 1 m. The smallest (<~50 μm) particles are moved by the wind as suspended dust, which may reach large heights (>100 m). Wind erosion can become a major problem whenever the soil is loose, dry, sandy and uncovered, while the wind speed exceeds the threshold velocity for initiation of particle movement (Sterk et al., 1999). It is a process which is influenced by the severity of the climate, the susceptibility (erodibility) of the soil and by the soil surface conditions (soil texture, soil roughness and soil cover). The wind removes not only soil particles, but also organic matter and nutrients, which reduces agricultural productivity in the source areas by declining the physical and chemical fertility of the topsoil (Zobeck and Fryrear, 1986). Besides soil degradation, wind erosion may cause direct crop damage (reduced quality and yields), pollute the atmosphere with fine particles, reduce visibility and cause deposition at unwanted places (roads, runaways, residential areas, etc.) with resulting economic costs (Mohammed et al., 1995).

Even though the process of wind erosion is often mentioned as one of the main soil degradation processes in Patagonia (e.g. Del Valle et al., 2010), few studies document how local conditions impact on wind erosion and aeolian sediment transport rates. To our knowledge, quantitative data of actual rates of aeolian sediment transport in Patagonia have never been published, and probably have not been determined either. Hence, the amount of soil which may be lost during Patagonian wind storms is generally unknown. For this study, it was hypothesised that clearance of natural vegetation from the Patagonian soils will increase the wind erosion risk, and requires technical measures to reduce the wind erosion amounts. Therefore, the aim of this study was to quantify aeolian sediment transport for a sandy soil in Central Patagonia. Specific objectives were as follows: 1) quantify the maximum aeolian mass fluxes from bare soil during Patagonian storms, 2) determine the potential reduction in wind erosion rates by an artificial windbreak, and 3) evaluate which sediment transport equation captures measured aeolian mass fluxes best.

2. Materials and methods

2.1. Site description

The research was carried out near Sarmiento in the Patagonian province Chubut. This province is located between the latitudes of 42 and 46° S covering an area of 224,686 km². The valley of Sarmiento is located in southern central Chubut (45° 32′ S, 69° 06′ W) at approximately 268 m above sea level, and covers an area of more than 50,000 ha. The valley is cut by the Río Senguer which connects two shallow lakes: Musters and Colhué Huapi. The area consists of extended flood plains with mainly sandy soils that have often a gravel layer below 1 m depth (Laya and Plunkett, 1983). The area is mainly covered by a particular type of vegetation known as "mallín", which consists of short grasses and small shrubs. Sheep and cattle are allowed to graze freely on the mallín. The surrounding area (outside the influence of the river) has the typical vegetation of the Patagonian steppe, which is dominated by bushes such as *Anarthrophyllum rigidum* and *Berberis buxifolia* (calafate).

The climate can be characterised as temperate or cold-temperate (mesothermal according to Thorntwaite, desertic according to Köppen) with mean annual temperatures varying between 8.2 °C and 13.5 °C. It is a dry area with on average only 150 mm of rain per year. Most of the precipitation occurs as snow during the winter (May to August). The strong prevailing westerly winds cause a phenomenon known as wind chill that makes the perceived mean annual temperature is lowered by 4.2 °C (Coronato, 1993). These effects are most pronounced during spring and summer (between September and January) when the wind reaches its maximum speeds. Most of the times (65–75% of daily observations) the winds blow from the West–Southwest. In the centre-west of Chubut, the mean annual values of wind speed are between 4.2 and 6.1 m s^{-1} (Paruelo et al., 1998).

A field experiment was conducted during a two-month campaign beginning late November 2008 and ending by the end of January 2009. The research was done on an 18 ha experimental cherry farm 'Bahía Solano' (45° 32′ S, 69° 05′ W), which was established in 2004. This farm is subdivided into 11 parcels of sizes ranging between 1.4 and 1.7 ha. The planting density of the cherry trees is 2222 trees per ha. Within the rows the cherry trees are spaced 1 m apart and the row spacing is 4.5 m. In the row middles *Festuca* spp. has been sown to protect the bare soil and is irrigated by sprinklers. This inter-row protection with *Festuca* spp. was only established 3 years after planting the cherry trees. The topography of the experimental site is flat, with a mean slope of 0.5%. The soils have a high sand content (>90%) and contain some gravel in the topsoil. There is a network of artificial windbreak systems and young natural windbreaks. The first are made out of nets 5 m high and with an optical porosity of 50%, while the second – mostly consisting of poplars (*Populus nigra* cv *italica*) – also reach heights of about 5 m. The optical windbreak porosities were estimated from digitised colour photographs using an image-processing programme (Zhang et al., 1995). The windbreaks are orientated North–south, perpendicular to the direction of the predominant westerly winds.

2.2. Wind speed and wind direction

Wind speed and wind direction were measured using a wind tower with 5 cup anemometers installed at different heights up to 4 m (0.5, 1.0, 1.5, 3.0 and 4.0 m) and a wind vane installed at a height of 5 m. The values were recorded and stored using a data logger (Campbell CR10) which provided average values of 1 min from reading intervals of 5 s. The tower was installed in an unsheltered area, free from disturbances, and provided the control conditions of the study. The wind speed values obtained were used to determine the friction velocity and the aerodynamic roughness height using the logarithmic wind profile (Stull, 1988):

$$U(z) = \frac{u_*}{\kappa} \ln\left(\frac{z}{z_o}\right) \quad (1)$$

where $U(z)$ is the average wind speed (m s^{-1}) at height z (m), z_o is the aerodynamic roughness length (m), κ is the Von Kármán constant (=0.4), and u_* is the friction or shear velocity (m s^{-1}). The latter is a

measure for the shear stress at the surface, and is defined as (Stull, 1988)

$$u_* = \sqrt{\tau_o/\rho} \quad (2)$$

where τ_o is the average shear stress (N m^{-2}) at the surface and ρ is the air density (kg m^{-3}). With two or more average wind speed measurements at different heights both u_* and z_o can be determined by linear regression.

2.3. Aeolian mass transport

Sediment transport was quantified using two saltiphones and 24 Modified Wilson and Cooke (MWAC) sediment catchers. The saltiphone (Fig. 1A) is an acoustic sensor that continuously records the impacts of saltating sand grains by means of a microphone with a membrane of 201 mm² installed inside a protective stainless steel tube (length = 130 mm, diameter = 50 mm). The tube is mounted on a ball bearing and has two wind vanes in the back which allow the saltiphone to be constantly oriented into the wind (Spaan and Van den Abeele, 1991). The centre of the microphone was installed at 0.1 m above the soil surface.

During storms, saltating particles moving through the tube hit the microphone producing high frequency signals. The saltating sand can be distinguished from other noises (e.g. wind, rain) by amplifying the signals and attenuating the low tones (Sterk et al., 1999). Each sand grain collision produces a signal that is cut off after 1 ms, meaning that in theory a maximum of 1000 grains per second can be recorded. But the actual number of grain impacts may be higher due to the overlap of collisions within the timeframe of the 1 ms pulses (Sterk et al., 1999). All the pulses were continuously counted and stored in the data logger at 1 min intervals thus giving a continuous monitoring of saltation transport rates. The output is in counts per minute and shows the temporal variability of the saltation process which can be used to determine the starting time, duration and the intensity of wind erosion events.

Twenty four MWAC sediment catchers (Fig. 1B) were used for the measurement of windblown mass fluxes. These devices consist of a series of sediment traps mounted on a rotating central pole. A wind vane (sail) is attached on the central pole ensuring a constant orientation in the wind direction. Each trap consists of a plastic bottle (100 ml) with two glass tubes (diameter = 8 mm, opening = 50.3 mm²) entering through the cap: an inlet tube which allows the entrance of air and sediment, and an outlet tube which allows air to escape (Sterk and Raats, 1996).

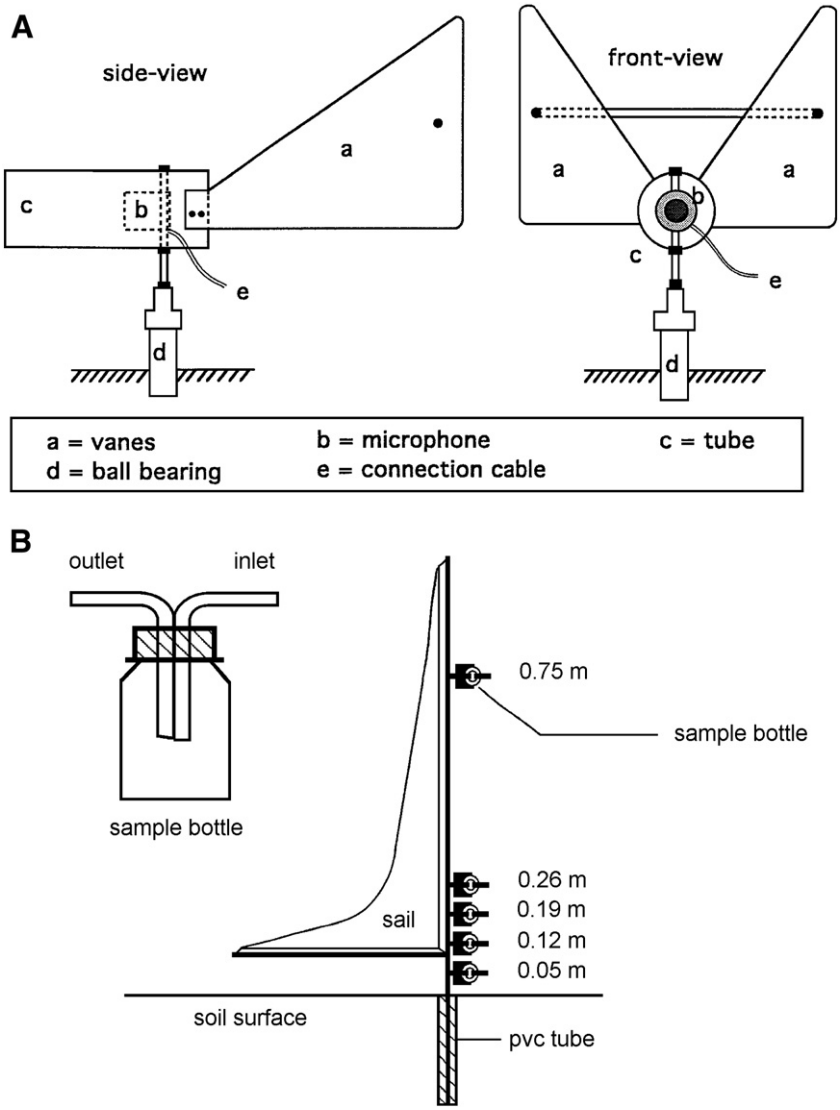

Fig. 1. Equipment used for measurement of wind erosion at Bahía Solana, Sarmiento, Argentina. A: the saltiphone, B: the Modified Wilson and Cooke sediment catcher (pvc = polyvinyl chloride).

Five traps were used on each catcher in order to trap moving aeolian material at 0.05, 0.12, 0.19, 0.26, and 0.75 m above the soil surface. Through the observations of the mass flux densities (kg m^{-2} s^{-1}) at one MWAC catcher and for one storm, a model was fitted describing the vertical profile of mass flux density (Zingg, 1953):

$$q(z) = q_o\left(\frac{z}{\alpha}+1\right)^{\beta} \quad (3)$$

where $q(z)$ is the horizontal mass flux density (kg m^{-2} s^{-1}) at height z (m); q_o is the mass flux density at $z=0$; α is a length scale (m); β is a dimensionless exponent. Integrating Eq. (3) over height from $z=0$ to $z=1$ m results in the measured mass flux below 1 m (Q in kg m^{-1} s^{-1}) at the sampling point. Correcting this value for the trapping efficiency provides a total mass flux (Q_t in kg m^{-1} s^{-1}) for each MWAC catcher. The overall trapping efficiency of the sediment catcher, defined as the ratio between the measured mass flux with a MWAC catcher (using Eq. (3)) and the actual mass flux measured in the wind tunnel was 54.4% (Sterk, 1993). Multiplying the total mass flux value with the duration of the wind event as recorded by the saltiphones will give a value of total mass transport (M in kg m^{-1}), equalling the total mass of aeolian sediment below 1 m height that passed a 1 m wide strip perpendicular to the average wind direction of the event.

2.4. Experimental setup

At the Bahía Solano field site, three transects of eight MWAC catchers were installed in plots with different degrees of wind exposure/shelter (Fig. 2). Two 100 by 20 m strips of land were cleared of the natural bush vegetation and levelled with a mouldboard plough. The plots were oriented West–east, parallel to the direction of the predominant erosive wind. One of the plots was protected by an artificial windbreak, oriented North–South, with an optical porosity of 50% and a height of 5 m at the non erodible boundary (NEB), which is the upwind edge of the plot where vegetation cover prevents aeolian sediment transport. The control plot was assumed to provide values of the maximum mass transport at the experimental site, while the protected plot provided information on the effect of the artificial windbreak on wind erosion. The MWAC sediment catchers were horizontally spaced across the plot at $x=1$, 5, 10, 20, 35, 50, 75, and 100 m, where x is the distance from the upwind edge. The wind tower and the saltiphones were installed in the control plot at $x=100$. One of the two saltiphones was placed next to the MWAC at $x=100$ m (Fig. 2).

The third transect of MWAC catchers was installed directly in the cherry orchard, with an artificial windbreak and a tree windbreak combined at the NEB. The tree windbreaks had an optical porosity of 25% and consisted of *P. nigra* trees with a canopy width of approximately 3 m and a height of about 5 m. Like the other transects, the cherry plot received an unobstructed wind flow while upwind roughness was similar to the roughness upwind of the other two plots (Fig. 2). In this case the catchers were placed at $x=1.8$, 8.8, 13.8, 18.8, 26.8, 40, 58, and 75 m due to the restriction of the distribution of the rows of the cherry trees.

2.5. Soil surface and sediment properties

Some soil surface properties which directly have an effect on wind erosion were determined for the experimental plots. Three topsoil (0–5 cm depth) samples were taken from each of the plots (at 2, 50 and 100 m from the NEB) and were analysed for soil texture using dry sieving and the Bouyoucos hydrometer method (Bouyoucos, 1936). Soil surface cover was estimated in the cherry orchard using the line-intercept method (Canfield, 1941). Stone cover was measured for both the control and the windbreak plots using the line-point intersect method (Bonham, 1989) whereby stone cover is being measured along a linear transect and is based on the number of "hits" on a rock or stone out of the total number of points measured along the transect. Moreover, the presence of soil crusts was estimated visually before and after erosion events. This was done because soil crusts are an important parameter to consider as their presence may reduce the quantity of windblown sediment by limiting the supply of saltation material (Sterk et al., 1999).

2.6. Wind erosion modelling

The data of total mass transport (M) recorded with the MWAC sediment catchers along the transects were fitted using a negative exponential decay curve (Stout, 1990). This curve describes the increase of mass transport from zero at the NEB to a maximum (M_{max}):

$$M(x) = M_{max}\left(1-e^{\frac{-x}{\varepsilon}}\right) \quad (4)$$

where x is the field length from the NEB (m); ε is a constant (m), a measure of the rate of increase of total mass transport; $M(x)$ is the total mass transport at field length x (kg m^{-1}); and M_{max} is the maximum total mass transport (kg m^{-1}) possible over the specific soil surface and for the wind conditions of the storm.

The maximum total mass transport (M_{max}) for a specific area and given wind conditions can be predicted with the use of various sediment transport equations. These equations calculate the maximum total mass flux ($Q_{t,max}$) which can be converted to the maximum total mass transport (M'_{max}) by multiplying it by the storm duration. Most sediment transport equations assume that the friction velocity

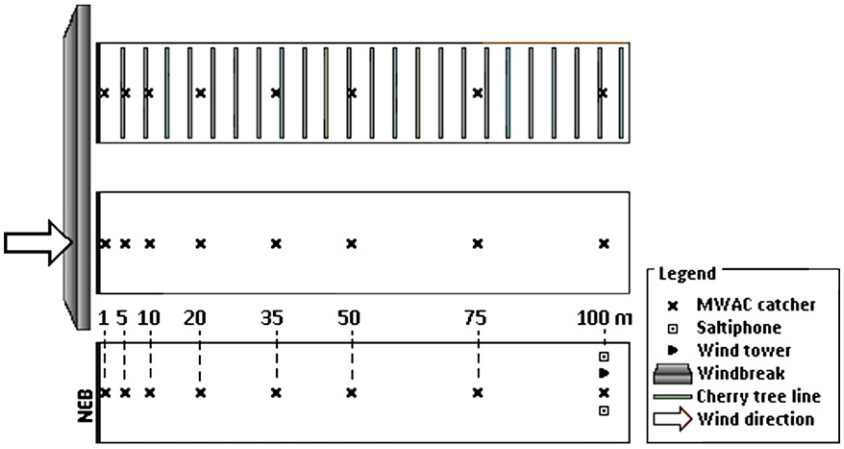

Fig. 2. Set up for the wind erosion experiment at Bahía Solana, Sarmiento, Argentina (NEB = Non Erodible Boundary).

Table 1
Overview of selected sediment transport equations used in this study.

Source	Transport equation[a]	Equation no.
Zingg (1953)	$Q_{t,max} = C_Z \left(\frac{d}{D}\right)^{0.75} \frac{\rho u_*^3}{g}$	(5)
Kawamura (1964)	$Q_{t,max} = C_{Ka}\left(1-\frac{u_{*t}}{u_*}\right)\left(1+\frac{u_{*t}}{u_*}\right)^2 \frac{\rho u_*^3}{g}$	(6)
Maegley (1976)	$Q_{t,max} = C_M \left(\frac{d}{D}\right)^{0.75}\left(1-\left[\frac{u_{*t}}{u_*}\right]^{13.72}\right)\frac{\rho u_*^3}{g}$	(7)
Kind (1976)	$Q_{t,max} = C_{Ki}\left(1-\left[\frac{u_{*t}}{u_*}\right]^2\right)\frac{\rho u_*^3}{g}$	(8)
Lettau and Lettau (1978)	$Q_{t,max} = C_L \left(\frac{d}{D}\right)^{0.5} \frac{\rho u_*^2}{g}(u_* - u_{*t})$	(9)

[a] $Q_{t,max}$ = maximum total mass flux (kg m^{-1} s^{-1}); C_Z, C_{Ka}, C_M, C_{Ki}, C_L = empirical coefficients (−); d = particle diameter (0.15 mm); D = 0.25 mm; ρ = air density (1.2 kg m^{-3}); g = gravitational acceleration (9.81 m s^{-1}); u_* = friction velocity (m s^{-1}); u_{*t} = threshold friction velocity (m s^{-1}).

(u_*) is the driving variable for sediment transport. Often equations also include the threshold friction velocity (u_{*t}) and incorporate the concept that movement of soil particles will only occur when u^* exceeds u_{*t}. The threshold friction velocity is the minimum friction velocity required to overcome the forces holding the particles on the surface (Shao, 2000). Furthermore, transport equations contain empirical constants that account for soil erodibility and are thus dependent on soil characteristics such as texture, soil moisture and soil cover.

Five transport equations (Table 1) were tested in order to fit maximum total mass fluxes ($Q_{t,max}$) to corresponding soil characteristics and recorded wind speed. Besides Eq. (5) in Table 1 all transport equations take the threshold condition into consideration; in other words, the mass transport rate will be zero when $u_* < u_{*t}$. The equation that does not take this factor into consideration will therefore predict sediment transport at velocities below those required to initiate particle movement. Hence for calculations using this method, the equation was only applied for wind conditions when $u_* > u_{*t}$.

The value for u_{*t} was estimated using data obtained from the saltiphones and corresponding wind profiles (Eq. (1)). This process is relatively simple and consists of taking the averages of the wind profile data over 30 min intervals. The summed saltiphone data for the same time intervals were plotted versus the 30 min u_* values. A linear regression equation provided an estimation of the u_{*t} value as being the intercept with the x-axis.

The equations were tested using data from the control plot only, because only for this plot measured values of u_* were available. Behind a windbreak the logarithmic wind profile (Eq. (1)) is not valid and no reliable u_* values could be obtained for the windbreak and cherry plots. The measured wind speed profiles and the total mass fluxes measured during 30 min intervals were used for curve fitting. The maximum total mass transport (M_{max}) obtained for a single event was divided by the storm duration to obtain ($Q_{t,max}$). This value was subsequently divided over 30 min intervals using the relative proportion of saltiphone counts during the same intervals. The curve fitting was done using the non-linear interpolation package of the SYSTAT statistical software package (Wilkinson, 1987). The goodness of fit (R^2) parameter was used to evaluate how well the different equations fitted the measured total mass fluxes for each individual storm. The overall predictive power of each sediment transport equation was also evaluated using the Nash-Sutcliffe model efficiency coefficient (Nash and Sutcliffe, 1970):

$$E = 1 - \frac{\sum\left(Q_{t,max}^{obs} - Q_{t,max}^{pred}\right)^2}{\sum\left(Q_{t,max}^{obs} - \overline{Q_{t,max}^{obs}}\right)^2} \quad (10)$$

where $Q_{t,max}^{obs}$ is the observed maximum total mass flux, $Q_{t,max}^{pred}$ is the modelled maximum total mass flux and $\overline{Q_{t,max}^{obs}}$ is the average of the observed maximum total mass fluxes. Values of E can range from −∞ to 1, with 1 meaning perfect match between observed and predicted values. An E-value equal to 0 means that the average of the observations is equally accurate as the model predictions. The Nash–Sutcliffe efficiencies were calculated by using the 30-minute observations of u^* and $Q_{t,max}$ of all storms combined.

3. Results

3.1. Wind storms and characteristics

A total of nine erosive storms was sampled during December 2008 and January 2009. A heavy rain event occurred during the storm of 20–21 December 2008 and small rain events also preceded the wind storm of 18–20 January 2009 and that of 24–26 January 2009. In the first case the rain clearly influenced the erodibility of the soil and it was therefore necessary to take this into consideration in the data analysis of this event. For the other two storms this was not done, as the saltiphone data did not clearly show any influence of the soil wetting on the saltation intensities.

The wind direction was quite constant throughout the entire experimental period. There were only few oscillations but the predominant direction was always West. The average wind direction throughout the experimental period was 270° ± 50°. The average wind direction recorded during wind erosion events was 275° ± 20°. Even though the wind speed fluctuated throughout the experimental period, the speeds were in general high, with an average of 5.9 m s^{-1} at 1.5 m height. Wind speed peaks of up to 20 m s^{-1} were observed during the very strong storm occurring on 20 and 21 December 2008.

The nine storms recorded during the experimental period showed nearly no variation in wind direction, but average wind speed and duration were variable (Table 2). In general storm duration was long, lasting from 4 up to 20 h. Wind direction varied between WSW (storm 8) and NW (storm 3) indicating the prevailing westerly

Table 2
Date, time, duration and wind characteristics of nine wind erosion events at Bahía Solana, Sarmiento, Argentina, during the period December 2008 to January 2009.

Date	Event	Time	Duration	Wind speed		Wind direction	
				Mean	SD	Mean	SD
		h:min	h.min	m s^{-1}	m s^{-1}	°	°
15–16 Dec.	1	12:49–04:27	15.38	7.88	1.2	275.8	12.1
16 Dec.	2	16:55–22:19	5.24	8.17	1.5	262.1	9.8
20–21 Dec.	3	18:11–04:55	10.44	13.23	2.5	314.6	14.8
23–24 Dec.	4	15:26–11:07	20.41	10.71	2.3	300.7	11.1
14 Jan.	5	14:02–16:40 19:58–23:32	6.12	11.10	1.2	256.1	10.7
15 Jan.	6	16:23–20:47	4.24	9.14	1.4	284.6	14.1
18–20 Jan.	7	23:07–04:36 02:39–08:51	11.41	9.61	1.4	258.7	12.7
20 Jan.	8	12:40–19:33	6.53	10.80	1.4	246.4	10.2
24–26 Jan	9	23:27–02:55 06:40–07:29	4.17	11.45	1.3	258.0	12.0

Table 3
Texture of the topsoil (0–5 cm) at Bahía Solano, Sarmiento, Argentina.

Site	No. of Samples	Particle size distribution[a]				
		Clay %	Silt %	Fine sand %	Medium sand %	Coarse sand %
Control	3	3.79	2.13	52.02	34.05	8.01
Windbreak	3	3.75	3.48	51.31	33.59	7.87
Cherry plot	3	4.43	3.08	51.15	33.48	7.86

[a] Clay: <2 μm; silt: 2–50 μm; fine sand 50–250 μm; medium sand 250–500 μm; coarse sand >500 μm.

direction of the wind. Moreover, the wind direction was nearly constant during specific storms, which is indicated by the low corresponding standard deviations (Table 2). The average wind speed of the storms varied from 7.9 to 13.2 m s^{-1} (measured at 1.5 m) and was also characterised by a low variation. The coefficients of variation of the wind speed varied between 10.8% and 21.5% for the nine storms. But these coefficients of variation are not really representing the turbulent nature of the wind storms. The sampling was done such that wind speed values for each minute were averages of 12 wind speed observations (sampling interval = 5 s). Hence, the turbulence occurring at higher frequencies was not captured. Leenders et al. (2005) measured wind speed during Sahelian storms at 8 Hz and obtained coefficients of variation varying between 21.7% and 26.3%.

3.2. Soil surface properties

Three soil samples were taken from each experimental site, one at the NEB, one at 50 m and one at 100 m from the NEB. All the topsoil samples were classified as sandy soils (Table 3), with the mean particle diameter falling within the fine sand class (0.05–0.25 mm). Initially, no stones were visible at the soil surface and the stone cover was assumed to be 0% for all three plots. During the experimental period, the stone cover in the cherry plot remained negligible, but in the control and windbreak plots it increased. The stone cover was measured by the line point-intersect method on the 7th of January in the control and windbreak plots. It was 41% in the control plot and 26% in the windbreak plot.

No pronounced soil crusting was observed during the entire experimental period. The sandy texture of the topsoil causes a low crusting potential. Only in one case was a thin crust observed in the control and windbreak plots. This crust was formed during the rainfall prior to the storm of 18–20 January 2009, but was quickly removed during the subsequent wind storm. During the experimental period, soil moisture content was low in the first few centimetres of the topsoil due to the constant presence of wind and intense sunshine that caused high evaporation rates. Soil moisture effects were therefore not included in this study. However, for a couple of storms soil moisture did decrease soil erodibility. But in only one case (Storm 3) was this effect strong enough to cause a lowering of mass transport in the early stages of the event, which was observed from the saltiphone recordings. Unlike the cherry plot, the control and windbreak plots had no vegetation cover during the experiment. The inter-row vegetation cover on the cherry plot as estimated by the line-intercept method was 34.3%.

3.3. Aeolian mass transport

In the cherry field no sediment transport was observed during the first three wind storms. The well established windbreak present at the upwind edge of the cherry field caused a reduction in the wind speed across the entire cherry field. Moreover, the 34.3% ground cover in the inter-row (*Festuca* spp.) protected the soil from wind erosion as it slowed down the wind and trapped saltating particles. The rows of cherry trees (perpendicular to the dominant wind direction) modify the wind profile by displacing it upwards from the surface to a new reference plane, the zero plane displacement height (Oke, 1978). As a result, the effective wind speed at ground level was reduced and the threshold friction velocity of particle movement was never exceeded by the friction velocity acting on the ground. Therefore it appears that the current orchard management and infrastructure are efficient in protecting the soil from wind erosion. The MWAC catchers were therefore removed from sector 2 in the cherry plantation zone and the experiment on the cherry field discontinued. Extra MWAC catchers were installed at 125 m from the NEB in the control site and in the windbreak site starting from the 13th of January 2009.

After each of the nine storms, the sediment in the MWAC traps was collected, dried, weighed and converted to mass flux densities. Eq. (3) then was fitted through the measured mass flux densities at five heights for each MWAC catcher and for each storm. A total mass flux (Q_t in kg m^{-1} s^{-1}) was calculated by integrating Eq. (3) over height and dividing by the trapping efficiency of the catchers. Multiplying Q_t with the storm duration resulted in the total mass transport values (M) for one specific storm event for each MWAC catcher (Table 4).

For each storm the negative exponential decay curve (Eq. (4)) was fitted through the M values for both the control and windbreak plots. In Fig. 3 the total mass transport profiles along the transects for the control and windbreak plots for different storm events are shown. The shapes of the curves in the control plot appear to be inconsistent. From previous studies (Sterk et al., 1999; Stout, 1990) the expected horizontal profiles should be similar to those obtained in storms 3, 5, and 9. This implies that the mass transport increases to a maximum value as the distance downwind from the NEB (or the windbreak) increases (negative exponential decay). This trend was also observed (though it was not as clear) in storms 7 and 8. However, in storms 1, 2, 4 and 6 there seems to be an exponential increase in mass transport as the distance from the NEB increases. This behaviour was not

Table 4
Aeolian mass transport values and soil losses during nine storms at Bahia Solana, Sarmiento, Argentina.

Storm	Duration	Control plot			Windbreak plot		
		M		Soil loss	M		Soil loss
		Mean	Range		Mean	Range	
	s	kg m^{-1}	kg m^{-1}	Mg ha^{-1}	kg m^{-1}	kg m^{-1}	Mg ha^{-1}
1	56,280	109.3	4.5–467.3	38.7	42.2	13.8–143.5	13.5
2	19,440	32.8	0.9–118.6	10.3	8.3	4.2–18.8	1.9
3	38,640	835.9	165.2–1581	148.7	472.8	202.1–991.4	85.8
4	74,460	94.7	7.0–346.5	27.4	34.6	11.8–88.4	8.8
5	22,320	44.2	7.3–84.1	6.4	28.8	10.9–65.5	3.7
6	15,840	20.2	4.6–45.6	3.6	15.3	5.5–28.0	2.0
7	42,060	7.9	1.2–17.9	1.6	6.7	3.3–12.2	0.8
8	24,780	30.6	2.5–76.3	6.0	16.3	7.1–31.9	2.3
9	15,420	31.7	2.6–62.8	4.9	16.9	4.0–34.2	2.5

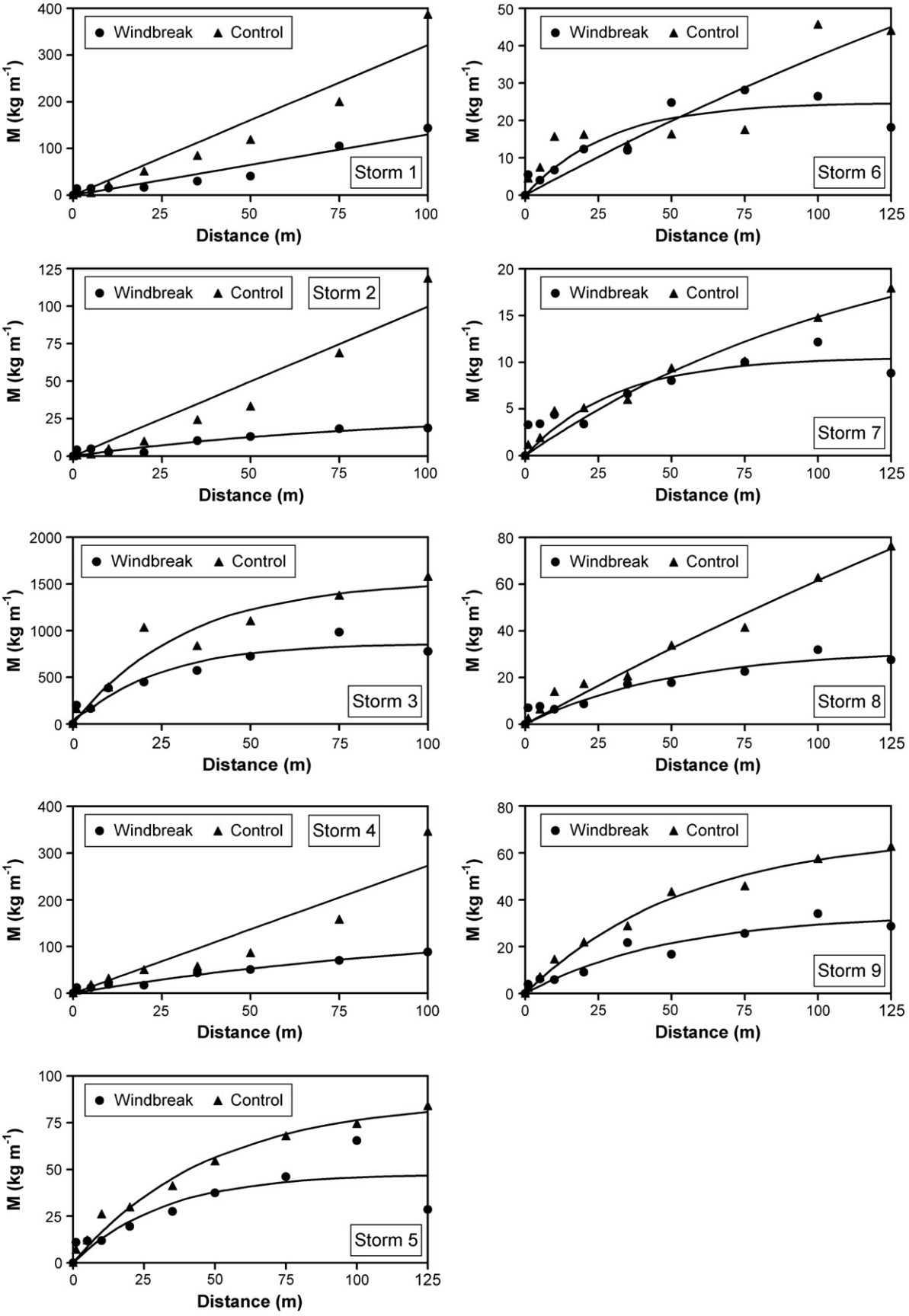

Fig. 3. Horizontal profiles of total mass transport (M) measured in a windbreak plot and a control plot during December 2008 and January 2009 at Bahía Solana, Sarmiento, Argentina.

observed in the windbreak plot, where the curves generally followed the exponential decay.

The strongest storm observed during the experimental period was storm 3. The wind speed reached values up to 20 m s^{-1} at 1.5 m and the resulting soil loss was 148.7 Mg ha^{-1} in the control plot and 85.8 Mg ha^{-1} in the windbreak plot. However, the erosion event was preceded by a rain and a hail storm which wetted the soil surface. Moisture causes cohesion between sand particles and thus increases the threshold velocity for soil particle movement (McKenna-Neuman and Nickling, 1989). Despite the wetting the aeolian mass transport was very intense during the storm, and it actually had a strong effect on subsequent conditions of the experimental plots. The storm was so strong that it increased the stone cover by blowing away most of the sandy material. This affected the soil erodibility and thus influenced the saltation transport of subsequent storms. It is quite clear from the range of values on the ordinates in Fig. 3 that the most intense storms were the first four, even though the average wind speed during the later storms was higher than during the first two storms (Table 2).

The change in erodibility in the plots can also be seen by comparing the saltation flux of two storms, one that took place before storm 3 (Fig. 4A) and one that took place after storm 3 (Fig. 4B). The saltation flux on 15–16 December 2008 reached higher peaks than the saltation flux on 14 January 2009 despite the higher wind speeds recorded during the latter. On 15–16 December 2008, significant saltation transport occurred at wind speeds between 10 and 12 m s^{-1}, while on 14 January 2008 a significant flux was recorded at wind speeds between 12 and 14 m s^{-1}. The protection of the soil created by the enhanced stone cover that resulted from the selective removal of sand particles during the third storm caused less saltation transport during subsequent storms. Hence, the increasing stone cover (from 0% to 41%) had a stabilising effect on the soil surface and reduced wind erosion. But this increase in stone cover was the result of previous wind erosion.

Windbreaks are a physical obstacle to advancing airflow and therefore reduce both wind speed for some distance upwind and downwind of the windbreak. The behaviour of the airflow in the lee of the windbreak is influenced by the porosity of the windbreak and the protected distance behind the windbreak is proportional to its height (h). The sheltered zone is between −5 h and 35 h (Vigiak et al., 2003). A reduction in wind speed was therefore expected in the windbreak plot, which would in turn cause a reduction in the total mass transport values. It is clear from the horizontal mass transport profiles (Fig. 3) that the artificial windbreak indeed provided protection against wind erosion. The total soil loss from the windbreak plot was reduced by 51.0% compared with the control plot. During storms 2 and 4 the highest reductions were observed, 81.6% and 67.9%, respectively. The lowest reductions recorded were 42.3% during storm 3 and 42.2% during storm 5. But, despite these reductions, the plot with the artificial windbreak still experienced a soil loss equal to 121.3 Mg ha^{-1}, which indicates that a single windbreak for a plot of a 100 m length is not sufficient to protect the soil from wind erosion. Multiple windbreaks or other protection measures are needed to reduce the soil loss to an acceptable level.

3.4. Threshold friction velocity

The threshold friction velocity (u_{*t}) was calculated using the friction velocities (u_*) based on 30 min values and their corresponding saltation fluxes in the same time intervals, as measured with the saltiphones. One u_{*t} was calculated for all the storms except for storm 3, which was influenced by the rain storm preceding the wind erosion event. The u_{*t} value for the other eight storms was calculated using the 30 min average wind profiles of each storm. These values were compiled and plotted against the respective saltation fluxes (Fig. 5). Based on a fitted linear regression equation through the data the threshold friction velocity was estimated to be 0.71 m s^{-1}.

Storm 3 was split into two parts, an initial wet part, followed by a later dry part when the wetted soil surface started to dry due to the strong wind. Fig. 6 shows the saltation flux and the u_* as a function of time for 30 min intervals during the third storm. The lines are discontinuous in order to differentiate two distinct periods of the storm: part 1 on the left and part 2 on the right. Initially, when the soil was wet and more cohesive, the calculated u_* values were fairly high (between 1.4 and 1.6 m s^{-1}) while the corresponding saltation flux was relatively low. This first part can be assumed to provide values for u_{*t} for wet-soil conditions (u_{*t} = 1.20 m s^{-1}). During the second part of the storm, when the soil became drier a much lower u_{*t} value was again obtained (u_{*t} = 0.76 m s^{-1}). The increase in the value of u_{*t} during the initial part of the third storm is similar to results obtained by Belly (1964)

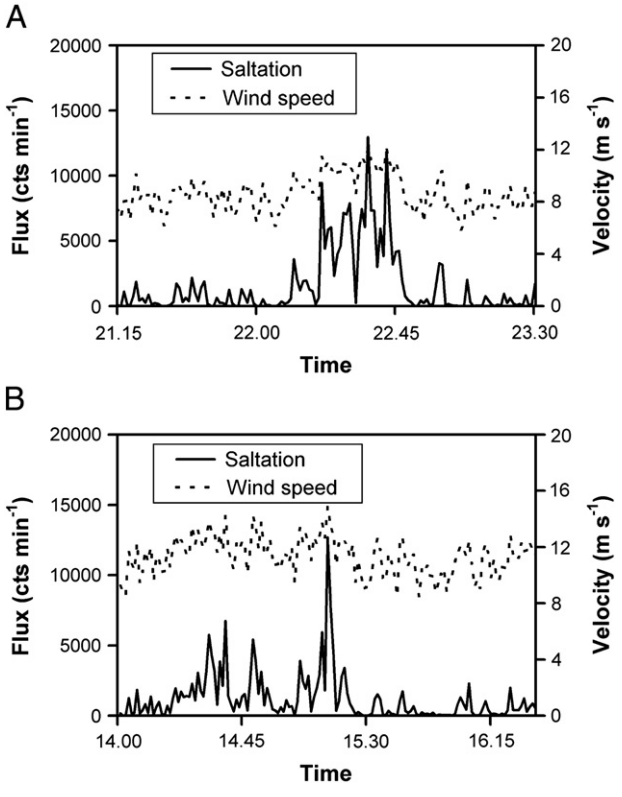

Fig. 4. Wind speed at 1.5 m and corresponding saltation flux at 0.1 m during the wind storms of the 15–16th December 2008 (A) and the 14th January 2009 (B) at Bahía Solana, Sarmiento, Argentina.

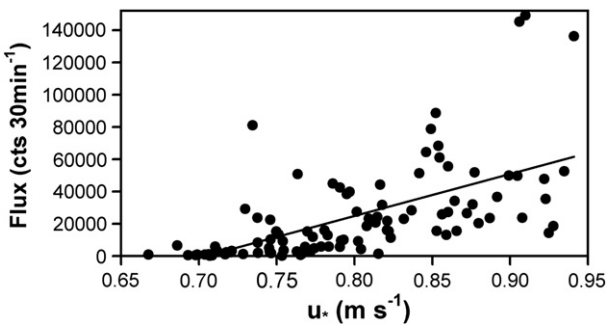

Fig. 5. Saltation flux plotted against the friction velocity of storms 5, 6, 7 and 9 at Bahía Solana, Sarmiento, Argentina.

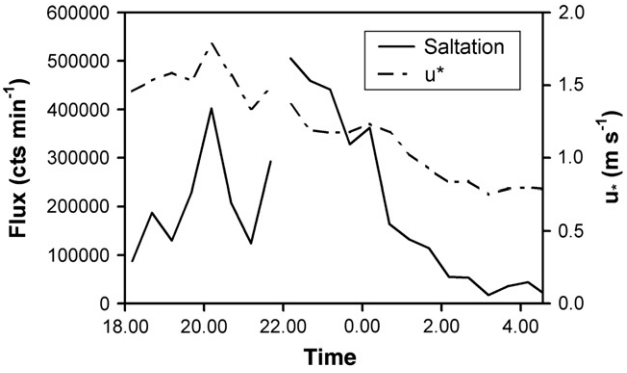

Fig. 6. Saltation flux and friction velocity (u^*) plotted against time for storm 3 at Bahía Solana, Sarmiento, Argentina. The first part of the storm represents wet conditions, while the second part represents dry conditions.

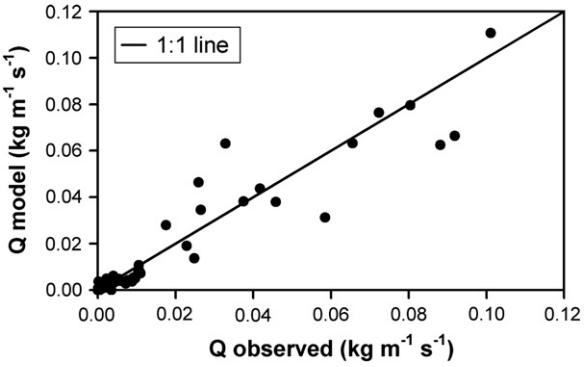

Fig. 7. Relation between measured and modelled total mass fluxes using the Kawamura (1964) sediment transport equation. Mass flux data were measured during five storms at Bahía Solana, Sarmiento, Argentina.

and Van Dijk et al. (1999). Belly (1964) found an average increase of 48% in u_{*t} when the gravimetric moisture content increased from 0 to 0.6%, and increases of up to 206% with moisture contents of up to 4%. Van Dijk et al. (1999) showed that u_{*t} increased on average by 35% on rainy days.

3.5. Fitting of sediment transport equations

Due to the unexpected horizontal mass transport profiles during storms 1, 2, 4 and 6, only storms 3, 5, 7, 8 and 9 were chosen to test the sediment transport equations listed in Table 1. One of the parameters that needed to be defined for the fitting of the transport equations is the mean soil particle diameter (d). Since the exact value of d was not available from the soil texture analysis, a value of 0.15 mm was used for the fitting of the transport equations. This value was calculated as the average size between the upper and lower limit of the main particle size class (0.05–0.25 mm) (Table 3).

Table 5 shows the C values of the fitted sediment transport equations through the 30 min data of u_* and the corresponding maximum total mass fluxes ($Q_{t,max}$) during the same time intervals. The R^2 values for the different fits indicate that the Zingg and Meagley sediment transport equations are less accurate than the other three equations. In general, the Kawamura, Kind and Lettau–Lettau equations gave good fits ($R^2 \geq 0.80$) for storms 3-dry and 8; reasonable fits ($0.40 \leq R^2 < 0.80$) for storms 3-wet, 5 and 7; and a poor fit ($R^2 < 0.40$) for storm 9. These R^2 values for the different sediment transport equations are similar to the range of R^2 values obtained by Leenders et al. (2011), who tested four different sediment transport equations during seven Sahelian wind storms. The tested sediment transport equations are all using wind speed instead of friction velocity as driving force, and were not considered in this study.

The Nash–Sutcliffe efficiency (Eq. (10)) was calculated using all observations of the six storms and ranged from 0.882 (Zingg) to 0.907 (Kawamura), showing that all tested sediment transport equations are good models for prediction of maximum total mass fluxes. The relation between the predicted and observed mass fluxes for the best performing equation (Kawamura) is shown in Fig. 7. Based on these findings and because the R^2 values for individual storms were also good, the Kawamura (1964) equation was selected for incorporation into a GIS-based model for predicting the effects of windbreaks on wind erosion in central Patagonia (De Sy, 2009).

It should be noted that the values of the C_{Ka} coefficients are variable (Table 5) due to the unique soil conditions during the storms. The C_{Ka} coefficient accounts for the erodibility of the soil and is a function of various parameters such as soil surface stone cover, soil moisture content and presence of a crust. The stone cover increased over time, which reduced the sediment transport and thus would lead to lower C_{Ka} values. Storm 7 and storm 9 were both preceded by days with rainfall events. Since soil moisture increases soil cohesiveness, calculated C_{Ka} values were lower (the soil was less erodible) for these storm events. The same applies to the third storm with a relatively high C_{Ka} when the soil was dry, and a lower C_{Ka} value when the soil was moist (less erodible). Furthermore, a thin crust was also observed on the soil surface before storm 7 occurred. This crust reduced the erodibility which is indicated by a lower C_{Ka} value.

The weight that these factors (stone cover, soil moisture, crusting) individually have on the C_{Ka} coefficient is not known. In this study two values of stone cover were obtained, 0 and 41% which had a respective C_{Ka} coefficient of 0.33 and 0.12. This means a 63.6% decrease in erodibility with a higher stone cover. However it is not known how the C_{Ka} coefficient behaves as the stone cover varies between these values. Increased soil moisture reduced the C_{Ka} coefficient, but the relation between soil moisture and the C_{Ka} coefficient could not be quantified because soil moisture was not measured. Similarly, the effect of surface crusting on the C_{Ka} coefficient was not quantified either. In order to have a correct estimation of the C_{Ka} coefficient, all of these factors have to be taken into consideration in future experimental set ups in order to calculate their weights on the C_{Ka} coefficient.

Table 5
Values of C coefficients for five sediment transport equations using 30 min data of total mass fluxes and u^* for five storms at Bahia Solana, Sarmiento, Argentina.

Storm	u_{*t}	Zingg		Kawamura		Maegley		Kind		Lettau–Lettau	
		C_Z	R^2	C_{Ka}	R^2	C_M	R^2	C_{Ki}	R^2	C_L	R^2
	m s^{-1}										
3 Wet	1.20	0.139	0.50	0.126	0.50	0.144	0.52	0.218	0.48	0.486	0.45
3 Dry	0.76	0.458	0.80	0.331	0.86	0.476	0.85	0.534	0.85	1.106	0.83
5	0.71	0.080	0.20	0.123	0.40	0.100	0.33	0.227	0.40	0.541	0.41
7	0.71	0.013	0.23	0.038	0.46	0.024	0.39	0.072	0.47	0.178	0.47
8	0.71	0.089	0.42	0.144	0.86	0.117	0.63	0.262	0.88	0.613	0.88
9	0.71	0.067	0.14	0.069	0.21	0.070	0.16	0.124	0.21	0.286	0.21

4. Discussion and conclusions

Despite the short duration of the experimental period (2 months) nine wind erosion events were recorded. Such number of storms is similar to Sahelian Africa, where about 12 severe wind storms occur during the early rainy season (mid May–end of July), but those storms generally have shorter durations (less than 1 h) (Michels, 1994; Sterk and Spaan, 1997). In general the Patagonian storms were intense (average wind speeds >7.9 m s^{-1}) and prolonged (4–20 h) (Table 2). The measured amounts of mass transport in the unprotected control plot were substantial (Table 4), especially during the first four storms. The total mass transport in the windbreak plot was on average reduced by 46.8%, while in the cherry plot, the wind break and the cherry trees provided sufficient protection to reduce the aeolian mass transport to negligible amounts.

The third storm on 20–21 December 2008 was extreme, with maximum measured values of total mass transport equal to 1581 kg m^{-1} in the control plot and 991 kg m^{-1} in the wind break plot. The highest wind speeds were recorded during this event, with peaks of up to 20 m s^{-1}(at 1.5 m height). Soil loss was equal to 148.7 Mg ha^{-1} from the control plot, and 85.8 Mg ha^{-1} from the windbreak plot, which translates to a loss of topsoil being equal to ~10 and ~6 mm, respectively. At the same time, the extreme erosion during this storm modified the soil erodibility conditions during subsequent events. The most erodible fraction of the soil was removed, leaving behind a surface with an increased stone cover. The non erodible stones reduced the wind erosion during the following storms, and during those storms the sediment transport rates were less intense despite similar wind conditions as the earlier storms. This process in which erodible soil particles are blown away, leaving behind a surface with non-erodible stones is similar to desert pavement development (Goudie, 2008). If the process can continue, a surface with nearly 100% stone cover can develop, which reduces further wind erosion to negligible levels. However, use of frequent mechanical tillage would result again in a loose sandy surface layer that continues to be prone to wind erosion.

The fitted exponential decay curve (Eq. (4)) through the measured mass transport values in the control plot showed unexpected patterns during four storms. Instead of reaching a maximum total mass transport value at a certain downwind distance, the curves continued to increase. Similar behaviour of horizontal mass flux profiles was observed by Davidson-Arnott and Law (1990), who measured aeolian sediment transport on a beach at Long Point, Lake Erie, Canada. In their study, horizontal mass flux profiles attained maximum values between 15 and 30 m downwind from the swash zone when wind speeds values were near the threshold value. However for higher wind speeds (>13 m s^{-1}) the mass flux profiles increased exponentially and did not reach a maximum mass flux within the width of the beach ($=35$ m). The behaviour of the mass flux profiles was clearly related to the average wind speed of the storm, but a physical explanation was not given by Davidson-Arnott and Law (1990). In the case of the Patagonian storms, the average wind speed cannot explain the observed behaviour. For instance, storm 6 showed an exponential increasing pattern, while storm 5 and 7 had expected profiles, even though their mean wind speeds were higher. Also changes in wind direction during the storms could not have played a role since the means of the storm wind directions were very similar, and no particular relationship could be detected.

A possible explanation for the observed exponential increase in mass transport along the experimental plot could be wind profile characteristics. As the wind proceeds over the natural vegetation, the wind profile is shifted upwards by the vegetation's roughness length. When the natural vegetation is abruptly interrupted by the bare strip of land, the wind profile changes in order to re-establish equilibrium with the new, lower roughness length. This has the effect of increasing the friction velocity at ground level from an initial low value at the NEB up to a new equilibrium value at a certain distance from the NEB (Kaimal and Finnigan, 1994). From the observed behaviour of the mass transport along the control plot during some storms it seems that the friction velocity did not reach a new equilibrium before the end of the plot was reached. However, it is not a completely satisfactory explanation as it was not observed for the other storms. Therefore, it appears that the unexpected behaviour in horizontal sediment transport profiles during four out of nine storms cannot be fully explained. Perhaps the turbulence characteristics during storms 1, 2, 4 and 6 were different and caused the unexpected behaviour, but the available wind speed data were not sufficient to conduct a turbulence analysis.

Although all the tested sediment transport equations fitted the measured total mass flux data well, the equation of Kawamura (1964) was considered the best performing model. This model expresses the total mass transport as a function of two empirical constants, the threshold friction velocity u_{*t} and the coefficient C_{Ka}. The C_{Ka} expresses the erodibility of the soil, which varied considerably per storm event. The fitted values ranged between 0.04 and 0.33. The parameter could therefore not be fixed to a generic site-specific parameter for all storms. Similar variability in the soil erodibility coefficient was also observed by Leenders et al. (in press), who conducted measurements of aeolian mass fluxes in northern Burkina Faso. They used the Radok (1977) sediment transport equation, which contains a similar soil erodibility factor. The factor was variable from storm to storm, and this variability was attributed to changing soil conditions (soil moisture, surface crusting and crop growth). It appears that using a more robust approach, C_{Ka} should be quantified as a function of different soil conditions that influence erodibility. Defining such function requires more detailed field experiments to determine the influence of soil conditions on C_{Ka}. In this case, data from more storms would be needed, and other factors that have a direct influence on the erodibility, such as stone cover, soil moisture and surface crusting, should be simultaneously monitored as well.

It is concluded that the Kawamura (1964) sediment transport equation can be effectively employed for capturing sediment transport dynamics for a specific storm event. However, the accurate prediction of sediment transport by this equation in Central Patagonia would require actual sediment transport measurements for fitting of the C_{Ka} and u_{*t} parameters, or a more precise documentation on the soil erodibility factors. Based on the findings of this study, the following Kawamura parameters can be recommended for application of the equation in Central Patagonia on a similar soil type without vegetation cover:

- Dry soil, no crust, zero stone cover: $u_{*t}=0.71$ m s^{-1}; $C_{Ka}=0.33$
- Wet soil, no crust, zero stone cover: $u_{*t}=1.20$ m s^{-1}; $C_{Ka}=0.13$
- Dry soil, no crust, stone cover 41%: $u_{*t}=0.71$ m s^{-1}; $C_{Ka}=0.14$
- Wet soil, no crust, stone cover 41%: $u_{*t}=1.20$ m s^{-1}; $C_{Ka}=0.07$

When crusting is a problem on the soil, the C_{Ka}values should be even reduced, but the data from this study are not sufficient to provide values for this factor. However, on such sandy soils crusting is usually not a serious problem.

Alternatively, a physically-based wind erosion model, such as the Wind Erosion Prediction System (WEPS; Hagen, 1991) could be used to calculate aeolian mass fluxes. However, application of such models is complicated and requires also detailed input data on wind field and soil characteristics. Visser et al. (2005) obtained reasonably good results when applying WEPS for an area in northern Burkina Faso, but the model application was based on data from an intensive field experiment.

This research shows that wind erosion poses a serious threat to sustained agricultural production of high value crops in agricultural valleys of Central Patagonia. The wind erosion risk is especially serious when the natural vegetation cover is removed from the sandy soils. Vegetation removal could be done by humans to clear areas

for arable land or fruit tree plantations. However, overgrazing by sheep may also result in reduced vegetation cover and thus increasing the risk of wind erosion (Peri and Bloomberg, 2002). Prior to land clearing for agricultural purposes it is advisable to establish windbreaks. The artificial windbreak tested in this study reduced the aeolian sediment transport by 46.8%, while the total soil loss was reduced by 51.0%. The very constant westerly wind direction during Patagonian storms makes windbreak design relatively easy, since using a North–south orientation is the most effective. But, the use of a single windbreak to protect a plot of a 100 m length is not sufficient. The measured soil loss from the windbreak plot was 121.3 Mg ha^{-1}, which is still very high. Additional windbreaks or other soil protection measures are needed to reduce soil losses to an acceptable level.

One of the peculiar aeolian features in the Central Patagonian landscape are the so-called Lenguas, which are narrow (~100–1000 m) strips of eroded soil running West–East through the landscape (Fig. 8A). These Lenguas can become quite long, exceeding 10 km, and some are visible on Google Earth (e.g. at 45° 17′ 30″ S, 70° 54′ 00″ W). These features usually originate at the shore of a lake where there is sand available which is transported through the landscape by the strong westerly winds. The saltating sand grains destroy the vegetation and create a bare surface that supplies more sand to the wind erosion process. After some time the upwind and central parts of the strip become a desert pavement (Fig. 8B) where the aeolian transport is reduced, and only dependent on the supply of sand at the source. But at the downwind end of the Lengua the process continues, increasing its length. The very constant westerly direction of the strong winds guarantees that these eroded strips remain narrow and become elongated. The Lenguas are scratches in the landscape and a direct result of the very strong westerly Patagonian winds.

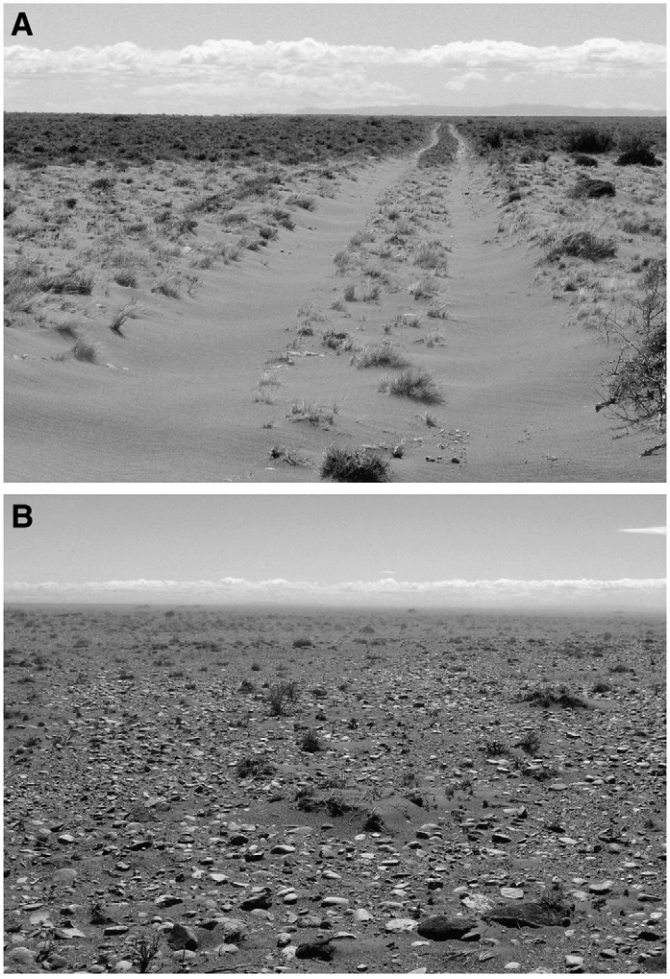

Fig. 8. (A) A Lengua in Central Patagonia—the picture shows the sharp boundary between the active aeolian (Lengua) surface and the stable surface where no wind erosion is occurring. (B) Heavily eroded surface inside a Lengua.

5. Acknowledgements

This work has been carried out as part of the EULACIAS INCO-dev Project, EU Sixth Framework Programme, Contract No. 0032387. We want to thank Sandra Szlápelis, Claudia Mundet, Cristina Esquivel, and Nora Baltuska from INTA for their assistance during the implementation of this study.

References

Bagnold, R.A., 1941. The Physics of Blown Sand and Desert Dunes. Methuen, London.
Belly, P.Y., 1964. Sand movement by wind. Technical Memorandum, no. 1, United States Army Corps of Engineers. Coastal Engineering Research Center, Vicksburg, Miss., USA.
Bonham, C.D., 1989. Measurements for Terrestrial Vegetation. Wiley, New York.
Bouyoucos, G.J., 1936. Directions for making mechanical analysis of soils by the hydrometer method. Soil Science 42, 225–230.
Canfield, R.H., 1941. Application of the line-intercept method in sampling range vegetation. Journal of Forestry 39, 388–394.
Cittadini, E.D., 2007. Sweet cherries from the end of the world: Options and constrains for fruit production systems in South Patagonia, Argentina. PhD Thesis, Wageningen University. Wageningen, the Netherlands.
Coronato, A., 1993. La Glaciación Moat (Pleistoceno Superior) en los Valles Pipo y Cañadón del Toro, Andes Fueguinos. XII Congreso Geológico Argentino, Actas VI, Mendoza, Argentina, pp. 40–47.
Coronato, F., Bisigato, A., 1998. A temperature pattern classification in Patagonia. International Journal of Climatology 18, 765–773.
Davidson-Arnott, R.G.D., Law, M.N., 1990. Seasonal patterns and controls on sediment supply to coastal foredunes, Long Point, Lake Erie. In: Nordstrom, K.F., Psuty, N., Carter, B. (Eds.), Coastal Dunes: Form and Process. Wiley, Chichester, UK, pp. 177–200.
De Sy, V., 2009. Spatial modelling of windbreak effects on wind erosion in South Patagonia, Argentina. Master thesis, Land Degradation and Development group, Wageningen University, Wageningen, the Netherlands.
Del Valle, H.F., Blanco, P.D., Metternicht, G.I., Zinck, J.A., 2010. Radar remote sensing of wind-driven land degradation processes in northeastern Patagonia. Journal of Environmental Quality 39, 62–75.
Dimitri, M.J., 1972. La Región de los Bosques Andino-Patagónicos. Colección Científica del INTA, Buenos Aires.
Goudie, A.S., 2008. The history and nature of wind erosion in deserts. Annual Review of Earth and Planetary Sciences 36, 97–119.
Hagen, L.J., 1991. A wind erosion prediction system to meet user needs. Journal of Soil and Water Conservation 46, 106–111.
Kaimal, J.C., Finnigan, J.J., 1994. Atmospheric Boundary Layer Flows: Their Structure and Measurement. Oxford Univ. Press, New York.
Kawamura, R., 1964. Study of sand movement by wind. Hydraulic Eng. Lab. Rep. Number HEL-2-8, Berkeley, University of California, pp. 99–108.
Kind, R.J., 1976. A critical examination of the requirements for model simulation of wind-induced erosion-deposition phenomena such as snow drifting. Atmospheric Environment 10, 219–227.
Laya, H., 1981. Levantamiento Semidetallado de Suelos. Formulación de un Plan Integral de Manejo Hídrico Para el VIRCh. CFI-Pcia. del Chubut, Convenio VIRCh, vol. 2. Trelew, Argentina.
Laya, H., Plunkett, S., 1983. Informe del reconocimiento edafológico en Sarmiento y Colhué Huapi. CORFO, Rawson, Chubut, Argentina.
Leenders, J., Van Boxel, J.H., Sterk, G., 2005. Wind forces and related saltation transport. Geomorphology 71, 357–372.
Leenders, J.K., Sterk, G., Van Boxel, J.H., 2011. Modelling wind-blown sediment transport around single vegetation elements. Earth Surface Processes and Landforms 36, 1218–1229.
León, R.J.C., Bran, D., Collantes, M., Paruelo, J.M., Soriano, A., 1998. Grandes Unidades de Vegetación de la Patagonia Extra Andina. Ecología Austral 8, 125–144.
Lettau, K., Lettau, H.H., 1978. Experimental and micro-meteorological field studies of dune migration, exploring the world's driest climate. IES Report 101, University of Winsconsin-Madison, Institute for Environmental Studies, Madison, USA, pp. 110–147.
Maegley, W.J., 1976. Saltation and Martian sandstorms. Reviews of Geophysics 14, 135–142.
McKenna-Neuman, C., Nickling, W.G., 1989. A theoretical and wind tunnel investigation of the effect of capillary water on the entrainment of sediment. Canadian Journal of Soil Science 69, 79–96.
Michels, K., 1994. Wind Erosion in the Southern Sahelian Zone: Extent, Control, and Effects on Millet Production. Verlag Ulrich E, Grauer, Stuttgart, Germany.
Mohammed, A.E., Stigter, C.J., Adam, H.S., 1995. Moving sand and its consequences on and near a severely desertified environment and a protective shelterbelt. Ari Soil Research and Rehabilitation 9, 423–435.

Nash, J.E., Sutcliffe, J.V., 1970. River flow forecasting through conceptual models, part I —a discussion of principles. Journal of Hydrology 10, 282–290.
Naumann, M., 1999. Pequeño Atlas Argentino con el Gran Chaco. Programa de Acción Nacional de Lucha contra la Desertificación: Cooperación Técnica Argentino-Alemana, p. 85 pp.
Oke, T.R., 1978. Boundary Layer Climates. Methuen, New York.
Paruelo, J.M., Beltrán, A., Jobbágy, E., Sala, O.E., Golluscio, R.A., 1998. The climate of Patagonia: general patterns and controls on biotic processes. Ecología Austral 8, 85–101.
Pelliza, A., Willems, P., Nakamatsu, V., Manero, A., 1997. Atlas dietario de herbívoros Patagónicos. Proyecto de Prevención y Control de la Desertificación para el Desarrollo Sustentable de la Patagonia (PRODESAR). Instituto Nacional de Tecnología Agropecuaria (INTA), and Deutsche Gessellschaft für Technische Zusammenarbeit, Bariloche, Argentina.
Peri, P.L., Bloomberg, M., 2002. Windbreaks in Southern Patagonia, Argentina: a review of research on growth models, wind speed reduction, and effects on crops. Agroforestry Systems 56, 129–144.
Radok, U., 1977. Snow drift. Journal of Glaciology 19, 123–139.
Shao, Y., 2000. Physics and Modelling of Wind Erosion. Kluwer Academic Publishers, London.
Soriano, A., 1992. Present conditions in the Patagonian Rangelands, in relation to potential impacts of a global change. Proceedings of the Workshop on Assessing Technologies and Management Systems for Agriculture and Forestry in Relation to Global Climate Change. Australian Government Publishing Service, Canberra, Australia, pp. 104–116.
Spaan, W.P., van den Abeele, G.D., 1991. Wind borne particle measurements with acoustic sensors. Soil Technology 4, 51–63.
Sterk, G., 1993. Sahelian Wind Erosion Research Project, Report III. Description and Calibration of Sediment Samplers. Dept. of Irrigation and Soil and Water Conservation, Wageningen Agricultural University, Wageningen, the Netherlands.
Sterk, G., Raats, P.A.C., 1996. Comparison of models describing the vertical distribution of wind-eroded sediment. Soil Science Society of America Journal 60, 1914–1919.
Sterk, G., Spaan, W.P., 1997. Wind erosion control with crop residues in the Sahel. Soil Science Society of America Journal 61, 911–917.
Sterk, G., López, M.V., Arrúe, J.L., 1999. Saltation transport on a silt loam soil in northeast Spain. Land Degradation & Devlopment 10, 545–554.
Stout, J.E., 1990. Wind erosion within a simple field. Transactions of ASAE 33, 1957–1960.
Stull, R.B., 1988. An Introduction to Boundary Layer Meteorology. Kluwer Academic Publishers, Dordrecht, the Netherlands.
Van Dijk, P.M., Arends, S.M., Van Boxel, J.H., 1999. Aeolian processes across transverse dunes II: modelling the sediment transport and profile development. Earth Surface Processes and Landforms 24, 319–333.
Vigiak, O., Sterk, G., Warren, A., Hagen, L.J., 2003. Spatial modeling of wind speed around windbreaks. Catena 52, 273–288.
Visser, S.M., Sterk, G., Karssenberg, D., 2005. Wind erosion modelling in a Sahelian environment. Environmental Modelling & Software 20, 69–84.
Wilkinson, L., 1987. SYSTAT: The System for Statistics. SYSTAT Inc., Evanston, IL, USA.
Zhang, H., Brandle, J.R., Meyer, G.E., Hodges, L., 1995. A model to evaluate windbreak protection efficiency. Agroforestry Systems 29, 191–200.
Zingg, A.W., 1953. Wind tunnel studies of the movement of sedimentary material. Proceedings of the 5th Hydraulic Conference, University of Iowa Studies in Engineering Bull., 34, pp. 111–135.
Zobeck, T.M., Fryrear, D.W., 1986. Chemical and physical characteristics of windblown sediment II. Chemical characteristics and total soil and nutrient discharge. Transactions of ASAE 29, 1037–1041.